Phase field modeling of deformation twinning in β-metastable titanium alloys

Juba HAMMA[a], Benoît APPOLAIRE[b], Yann LE BOUAR[a], Alphonse FINEL[a]

[a]Laboratoire d'Etude des Microstructures (LEM), ONERA, CNRS, Université Paris-Saclay F-92332, Châtillon, France

[b] Université de Lorraine-CNRS, IJL, Campus Artem, 54000, Nancy, France

Abstract

A multi-phase field model describing the anisotropic growth of the {332}<113> twinning system in β-metastable titanium alloys is hereby presented considering the geometrically linear and non-linear frameworks. Phase fields are associated with each twin variant of the {332}<113> system. The lattice transformation describing the twinning systems is incorporated in the model via relevant eigenstrain tensors. We illustrate the capability of our model by investigating the formation of twins networks, within both geometrically linear and non linear frameworks. In particular, it is shown that the predicted microstructures exhibit strong differences, resulting from a difference in the selection of the variant habit planes.

1. Introduction

Recently, new β-metastable titanium alloys have been developed that combine TRIP and TWIP behaviors (TRIP for TRansformation Induced Plasticity and TWIP for TWinning Induced Plasticity). They display improved mechanical properties, such as high strength (up to 1200 MPa in Ultimate Tensile Strength) and ductility of about 45% at fracture, accompanied by an unprecedented strain hardening for titanium alloys at ambient temperature [1,2]. These mechanical properties are attributed to very complex microstructures engendered by the mechanical destabilization of the initial bcc phase (β) in the course of the deformation [3]. Indeed, the microstructure features numerous twins following the peculiar {332}<113> twinning mode of the β phase, specific to β-titanium alloys, as well as orthorhombic (α") and simple hexagonal (ω) phases ensued from concomitant displacive transformations. Moreover, experimental observations revealed the possible activation of secondary deformation mechanisms, i.e. twins and/or α" phase inside primary twins of the β phase [1-3].

In order to better understand the formation of the complex microstructures described above, we propose a numerical model using the phase field method. This method provides a thermodynamically consistent framework to couple the mechanisms at the origin of the microstructure evolution. As a first step, we focus only on the {332}<113> twinning system. Contrary to recent works using phase field methods to investigate deformation twinning [4-7], we do not resort on an anisotropic twin boundary energy to control the shape of the twins, but rather investigate the importance of the framework for mechanics, i.e. either geometrically linear or non-linear. The capabilities of of the model to describe the {332}<113> anisotropic twin growth is illustrated on a simple configuration, and the importance of considering a geometrically non-linear framework is addressed.

2. Phase field model

The model is based on the introduction of twelve phase fields $\varphi_v(r)$, with $v \in 1;12$, corresponding to the twelve {332} twin variants. We consider that $\varphi_v(r) = 0$ when r is within the initial bcc grain, called matrix for simplicity, and that $\varphi_v(r) = 1$ when r is within twin variant v. The total free energy $\mathcal{F}_{tot}$ that depends on the phase fields is additively split into two contributions: $\mathcal{F}_{tot} = \mathcal{F}_{int} + \mathcal{F}_{elas}$.

The first contribution $\mathcal{F}_{int}$ is the free energy associated with the twin boundaries. It is written as:

$$\mathcal{F}_{int} = \int_\Omega \left(\sum_{v=1}^{n} W \, \varphi_v^2 (1-\varphi_v)^2 + \frac{\alpha}{2} |\nabla \varphi_v|^2 \right) dV \tag{1}$$

where the first term is the usual double-well potential of amplitude W, which discriminates the two states of the microstructure (twin variant v or matrix). The second term is a gradient squared, which enforces the fields to remain smooth. Both α and W can be related to the twin boundary energy and thickness. In this work, an isotropic twin boundary energy is considered.

Considering a geometrically non linear framework, the elastic energy reads:

$$F_{elas}^{NL} = \int_\Omega \frac{1}{2} C_{ijkl} \, E_{ij}^e \, E_{kl}^e \, dV \tag{2}$$

with

$$E_{ij}^e = \frac{1}{2} \left(F_{mi}^e F_{mj}^e - \delta_{ij} \right) \tag{3}$$

and

$$F_{ij}^0 = \delta_{ij} + \sum_{v=1}^{n} h(\varphi_v) \, \gamma_{tw} \, \left(\eta_i^v \, K_j^v \right) \tag{4}$$

C_{ijkl} are the elastic constants of the material. E^e is the Green-Lagrange elastic strain tensor related to the total deformation gradient F by the usual multiplicative decomposition F=$F^e F^0$ between an elastic contribution F^e and an inelastic one F^0. The tensor F^0 interpolates between the stress-free shear of the twin variants using a monotonous polynomial function $h(\varphi) = \varphi^3(6\varphi^4 - 15\varphi + 10)$.

© The Authors, published by EDP Sciences. This is an open access article distributed under the terms of the Creative Commons Attribution License 4.0 (http://creativecommons.org/licenses/by/4.0/).

The stress-free shear of a given variant v is related to the vector normal to the twinning plane K^v, the twinning direction η^v and the shear strain amplitude γ_{tw}. In the case of the {332}<113> twinning system, $\gamma tw = 0.35$, and K^v is the unit vector perpendicular to one of the twelve {332} planes and η^v the unit vector along the corresponding <113> direction. In the present work, elastic constants are assumed isotropic to focus on the anisotropy induced by the stress-free twin shear tensor.

Now assuming a geometrically linear framework, the elastic energy reads:

$$\mathcal{F}^L_{elas} = \int_\Omega \frac{1}{2} C_{ijkl}\, \varepsilon^e_{ij}\, \varepsilon^e_{kl} dV \tag{5}$$

with

$$\varepsilon^e_{ij} = \left(\varepsilon_{ij} - \varepsilon^0_{ij}\right) \tag{6}$$

and

$$\varepsilon^0_{ij} = \sum_{v=1}^{n} h(\varphi_v) \frac{\gamma_{tw}}{2} \left(\eta^v_i\, K^v_j + K^v_i\, \eta^v_j\right) \tag{7}$$

ε^e is the linearised strain tensor and ε the total strain tensor. The eigenstrain tensor ε^0 plays the same role as stress-free twin shear tensor F^0.

The non-conserved phase fields follow a simple dissipative dynamics:

$$\frac{\partial \varphi_v}{\partial t} = -L \frac{\delta \mathcal{F}}{\delta \varphi_v} \tag{8}$$

where $\frac{\delta}{\delta \varphi_v}$ stands for the variational derivative with respect to the field φ_v, and L is a positive coefficient assumed constant.

Static mechanical equilibrium is assumed. In the geometrically non-linear framework, it is expressed as:

$$\frac{\partial}{\partial x_j}\left(\frac{\delta F_{elas}}{\delta F_{ij}}\right) = \frac{\partial P_{ij}}{\partial x_j} = 0 \tag{9}$$

where P is the first Piola-Kirchhoff stress tensor.

In the geometrically linear framework, the static mechanical equilibrium reads:

$$\frac{\partial}{\partial x_j}\left(\frac{\delta F_{elas}}{\delta \varepsilon_{ij}}\right) = \frac{\partial \sigma_{ij}}{\partial x_j} = 0 \tag{10}$$

where σ is the Cauchy stress tensor.

In both cases, mechanical equilibrium is solved using spectral methods [8,9]. Periodic boundary conditions and average applied strain, $\langle F \rangle$ or $\langle \varepsilon \rangle$, are considered in the present work.

3. Results and discussion

Our phase field model is now applied to the growth of two specific variants of the {332}<113> twinning system that are usually observed to form particular networks (e.g. [2]). For that purpose, we associate two phase fields with the two variants featuring two different eigenstrains. Fig. 1 compares the evolution of the variants predicted by the two frameworks for elasticity, i.e geometrically linear and non-linear.

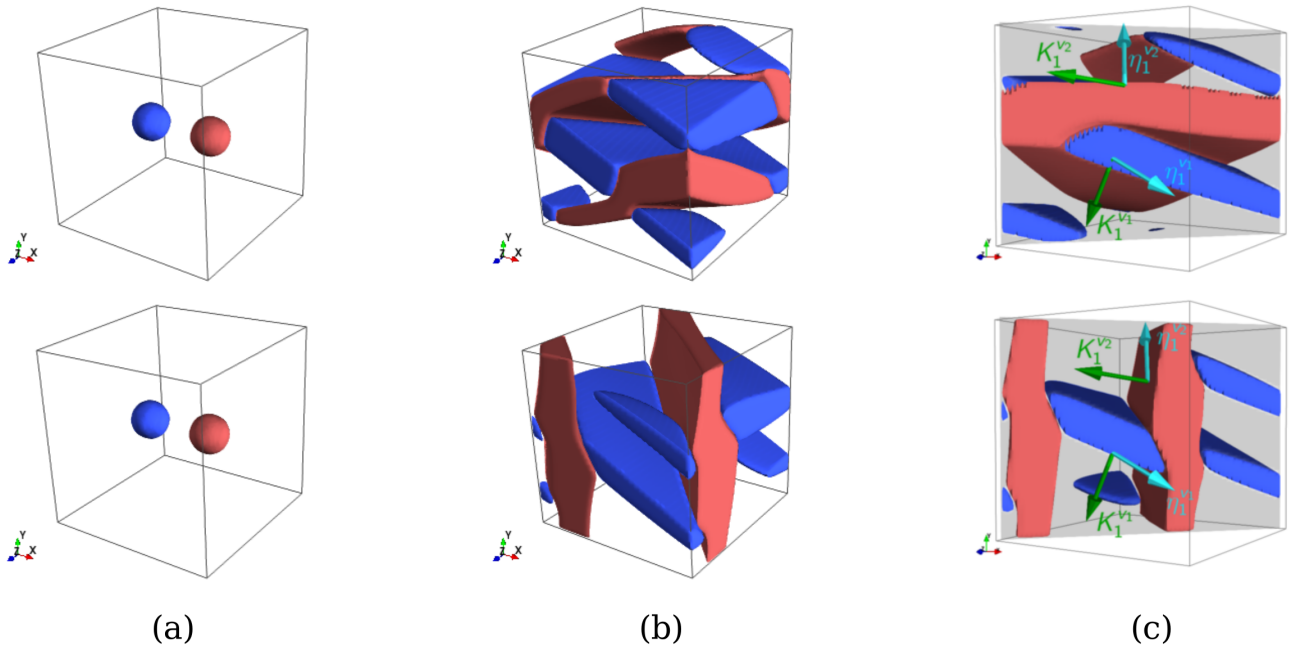

Fig. 1 : Evolution of two twin variants (red and blue) in the geometrically linear (upper row) and non-linear (lower row) frameworks. (a) Initial condition. (b) Final microstructure obtained after 50000 (upper row) and 10000 (lower row) time steps. (c) Grey planes are (101) sections of the final microstructure. Theoretical twinning planes are indicated by green arrows (K_1) and twinning direction by cyan arrows (η_1).

As initial condition, two spherical nuclei of different variants have been included at respectively $(L/4, L/2, L/2)$ and $(3L/4, L/2, L/2)$ where L is the size of the simulation box (Fig. 1a). The following constant average strain or deformation gradient is applied:

$$\langle \varepsilon \rangle = \gamma_{app} \begin{pmatrix} 0 & 1 & 0 \\ 1 & 0 & 0 \\ 0 & 0 & 0 \end{pmatrix} \qquad \langle F \rangle = \begin{pmatrix} 1 & \gamma_{app} & 0 \\ \gamma_{app} & 1 & 0 \\ 0 & 0 & 1 \end{pmatrix} \tag{11}$$

with $\gamma_{app} = 0.05$.

Fig. 1b shows the predicted microstructures obtained in the linear and non-linear frameworks. In both cases, the nuclei grow to adopt rapidly plate shapes, with different habit planes associated with the different variants, driven by the elastic energy minimization. Due to periodic boundary conditions, the growth of the plates gives rise to networks of twins. Interfaces between the two variants exhibit particular orientations that differ from the habit planes.

The networks are different depending on the way elasticity is handled: whereas blue twins display the same orientation within the linear and non-linear geometry, the red twins adopt habit planes that differ between the two geometries. This is clearly visible in Fig. 1c, where (101) sections of the microstructure are shown. In the nonlinear framework, the habit plane of the red twins complies with the theoretical twinning plane K_1^{v2}, containing the twinning direction η_1^{v2} as expected and experimentally observed (e.g. [10,11]). It is worth noting that the deflections of the red habit plane in contact with blue twins are also systematically observed in micrographs.
On the contrary, in the linear framework, the red twins display habit planes that are *perpendicular* to the theoretical shear direction and *parallel* to the theoretical normal direction. The resulting network is therefore very different from what is observed experimentally.

The strong difference in the twin patterns between both frameworks can be explained by the importance of the rotations involved in the twinning process, as already investigated in the case of martensitic transformations [12]. Indeed, a 10° rotation is involved in the simple shear (F^0) describing the twinning process. Whereas this rotation does not contribute to any increase in the elastic energy in the geometrically nonlinear framework (F^{NL}_{elas} is rotation invariant, see Eqs. (5-6)), it is not the case for the linear framework. As a consequence, the linear framework predicts that two orthogonal habit planes are possible when the nonlinear framework relaxes this degeneracy and only favors the theoretical K_1 habit plane. Hence, the flaw of the linear framework induces the possible selection of a wrong habit plane, as shown in Fig. 1c upper row. It can be concluded that a proper description of deformation twinning featuring different variants must rely on the geometrically nonlinear framework.

4. Conclusion

A phase field model that reproduces the growth of {332} twin variants was hereby proposed considering the geometrically linear and nonlinear frameworks respectively. Both models reproduce the anisotropic growth of twin without introducing interface energy anisotropy. In other words, the elastic energy anisotropy introduced here via the eigenstrain tensors is at the origin of the plate-like twins. However, the results showed that the use of the geometrically linear framework generates the growth of unacceptable twin variants in the system, giving rise to microstructures that might be acceptable at first sight, but totally different from the experimental results.

5. References

[1] Sun, F., Zhang, J. Y., Marteleur, M., Brozek, C., Rauch, E. F., Veron, M., Vermaut, P., Prima, F., Scripta Materialia 94 (2015) 17-20.

[2] Min, X. H., Tsuzaki, K., Emura, S., Tsuchiya, K., Materials Science and Engineering: A 554 (2012), 53-60.

[3] Marteleur, M., Sun, F., Gloriant, T., Vermaut, P., Jacques, P. J., Prima, F., Scripta Materialia 66 (2012), 749-752.

[4] Heo, T. W., Wang, Y., Bhattacharya, S., Sun, X., Hu, S., Chen, L.-Q., Philosophical Magazine Letters 91 (2011), 110-121.

[5] Liu, H., Lin, F. X., Zhao, P., Moelans, N., Wang, Y., Nie, J. F., Acta Materialia 153 (2018), 86-107.

[6] Clayton, J.D, Knap, J., Physica D 240 (2011), 841-858.

[7] Liu, C., Shanthraj, P., Diehl, M., Roters, F., Dong, S., Dong, J., Ding, W., International Journal of Plasticity 106 (2018), 203–227.

[8] Boussinot, G., Le Bouar, Y., Finel, A., Acta Materialia 58 (2010), 4170-4181.

[9] Kabel, M., Böhlke, T., Schneider, M., Computational Mechanics 54 (2014), 1497-1514.

[10] Lai, M. J., Tasan, C. C., Raabe, D., Acta Materialia 111 (2016), 173-186.

[11] Chen, B., Sun, W., Scripta Materialia 150 (2018), 115-119.

[12] Finel, A., Le Bouar, Y., Gaubert, A., Salman, U., Comptes Rendus Physique 11 (2010), 245–256.